ADVANCED BIOSYSTEMS
www.adv-biosys.com

Template Curvature Influences Cell Alignment to Create Improved Human Corneal Tissue Equivalents

*Ricardo M. Gouveia, Elena Koudouna, James Jester, Francisco Figueiredo, and Che J. Connon**

To accurately create corneal stromal equivalents with native-like structure and composition, a new biofunctionalized, curved template is developed that allows the precise orientation of cells and of their extracellular matrix. This template is the first demonstration that curvature alone is sufficient to induce the alignment of human corneal stromal cells, which in turn are able to biofabricate stromal tissue equivalents with cornea-like shape and composition. Specifically, tissues self-released from curved templates show a highly organized nanostructure, comprised of aligned collagen fibrils, significantly higher expression of corneal stroma-characteristic markers keratocan, lumican, decorin, ALDH3, and CHST6 ($p = 0.012$, 0.033, 0.029, 0.003, and 0.02, respectively), as well as significantly higher elastic modulus ($p = 0.0001$) compared with their planar counterparts. Moreover, curved tissues are shown to support the growth, stratification, and differentiation of human corneal epithelial cells in vitro, while maintaining their structural integrity and shape without any supporting carriers, scaffolds, or crosslinking agents. Together, these results demonstrate that corneal stromal cells can align and create highly organized, purposeful tissues by the influence of substrate curvature alone, and without the need of additional topographical cues. These findings can be important to further understand the mechanisms of corneal biosynthesis both in vitro and in vivo.

1. Introduction

The creation of corneal stromal equivalents, particularly using natural components, typifies many of the challenges in tissue engineering. Necessarily, a suitable corneal stromal substitute needs to be biocompatible, mechanically stable, and optically transparent, as well as capable of resisting contraction and proteolytic degradation before and after tissue transplantation.[1] To date, some of the most promising substitutes are represented by collagen-based scaffold materials, which, once crosslinked, are shown to be usable as long-term corneal stromal replacements (as previously reviewed).[2] Typically, these materials were used in a top-down approach, with an initial step of hydrogel formation, followed by cell seeding, and matrix rearrangement after grafting.[3–5] More recently, however, corneal stromal tissues have been engineered in vitro by means of bottom-up strategies using the cells themselves to generate the matrix, i.e., comprise aligned collagen fibrils, and thus recreate the well-defined, 3D microarchitecture of the native organ.[6] This cell-induced structural anisotropy represented an important feature, as it fundamentally contributes to the very particular mechanical, optical, and functional properties of the human cornea.[7]

The alignment of collagen fibrils has been achieved in vitro using multiple strategies, including electrospinning,[8] molecular crowding,[9,10] magnetic orientation,[11] thin-film confinement,[12] and fluid shearing.[13] Preferably, though, the regulation of collagen anisotropy within engineered tissues should be accomplished by mimicking in vivo conditions and allowing cells within such tissues to remain viable. In this context, tissue templating presents several advantages over other methods, as it can direct cells to align, and in turn produce their own aligned collagen matrix,[14–16] as well as promote easy tissue recovery with minimal manipulation.[17] To this purpose, we recently used a tissue-templating approach based on polytetrafluoroethylene nanogrooves to direct the orientation of corneal stromal cells and of their deposited matrix.[18] Moreover, we combined this system with a smart peptide amphiphile (PA) coating to instruct corneal stromal cells to biofabricate and subsequently self-release stromal connective tissue[19] while

Dr. R. M. Gouveia, Prof. F. Figueiredo, Prof. C. J. Connon
Institute of Genetic Medicine
Newcastle University
Newcastle upon Tyne NE1 3BZ, UK
E-mail: che.connon@newcastle.ac.uk
Dr. E. Koudouna, Prof. J. Jester
Gavin Herbert Eye Institute
University of California Irvine
Irvine, CA 92697, USA
Dr. E. Koudouna
Structural Biophysics Research Group
School of Optometry and Vision Sciences
Cardiff University
Cardiff CF24 4HQ, Wales, UK
Prof. F. Figueiredo
Department of Ophthalmology
Royal Victoria Infirmary
Newcastle upon Tyne NE1 4LP, UK
The ORCID identification number(s) for the author(s) of this article can be found under https://doi.org/10.1002/adbi.201700135.

DOI: 10.1002/adbi.201700135

rationally designing collagen fibril alignment.[20] These corneal stromal tissue equivalents were shown to be highly transparent, robust, capable of supporting corneal epithelial cell growth, and safe graft materials.[21] However, these tissues lacked the natural curvature of the cornea.

Strategies to recreate cornea-shaped (geometrically curved) stromal tissue equivalents are still rare and mostly based on the production of collagen-based curved gels, to which cells are subsequently added.[22,23] Alternatively, mechanical strain has been used to induce spherical curvature on planar collagen hydrogels containing corneal stromal cells.[24] Current bottom-up templating systems are still restricted to produce planar tissues. As such, in the present study we developed a new curved template that supported the biofabrication of cornea-shaped stromal tissue equivalents. Importantly, we found that surface curvature was in and of itself sufficient to induce human corneal stromal cells to align and subsequently deposit highly organized extracellular matrix (ECM) to form cornea-shaped stromal tissue equivalents. These results illustrated, for the first time, the potential use of a simple topographical cue (i.e., curvature) to direct cell alignment and phenotype. Moreover, they pave the way to the creation of sophisticated corneal tissue substitutes with purposeful application in tissue engineering and regenerative medicine.

2. Results

In order to create cornea-shaped tissue equivalents via a bottom-up approach, we developed novel template designs with a curved geometry (**Figure 1**a). First, lens-shaped agarose gels were cast using glass molds (Figure S1, Supporting Information) and subsequently mounted in tissue culture plates using a thin extra layer of agarose (Figure 1a). This method showed to have three advantages: it secured the curved agarose gels in place; it created a flat region surrounding the curved templates where cells could be initially seeded; and guaranteed a smooth sloped transition (of ≈26°) between the flat and curved surfaces, thus easing cell migration upward on to the curved templates (Figure 1a). Planar agarose templates were similarly created and used as controls for the effect of template geometry

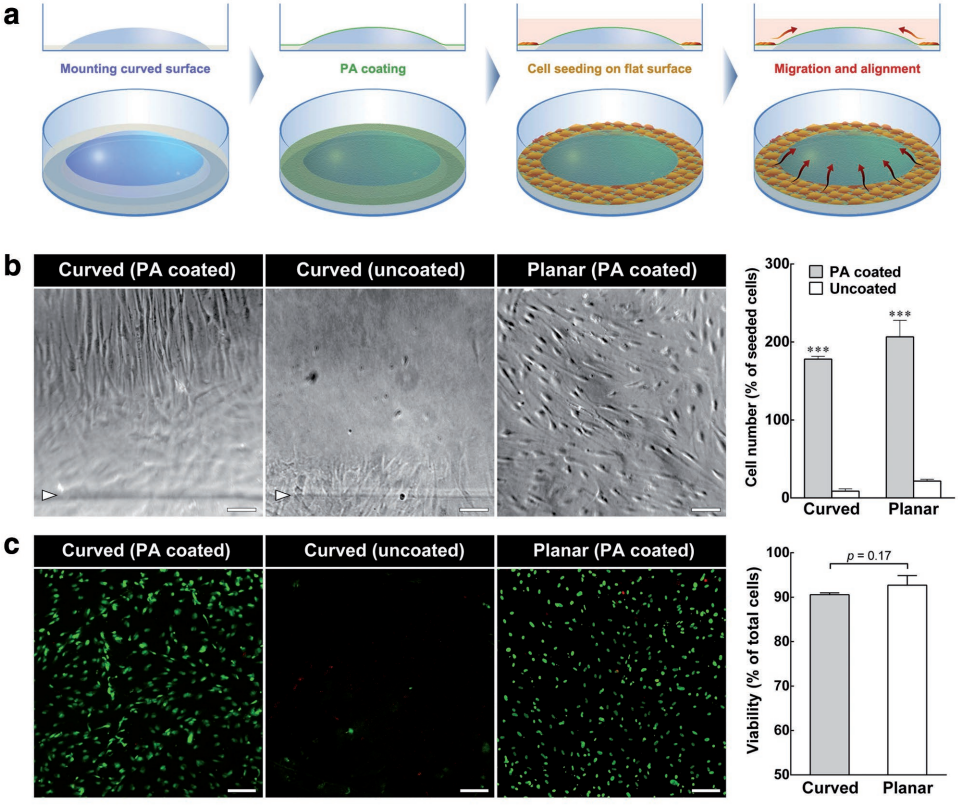

Figure 1. Adhesion and migration of human corneal stromal cells on to curved templates. a) Schematic representation of cell culture setup using PA-coated curved templates. Curved surfaces were mounted into tissue culture plates, embedded in a flat layer of agarose, and then coated with cell adhesive PA. Cells seeded onto the flat surface at the periphery of the wells were allowed to adhere and then migrate up toward the center of the templates. Templates comprising planar surfaces only (different geometry) or curved surfaces left uncoated (different bioactivity) were used as negative controls. b) Representative phase-contrast micrographs of PA-coated and uncoated curved and planar agarose templates. Cells were able to migrate from the flat regions of the template, through the flat-curved interface (arrowheads), and up toward the center of PA-coated, but not uncoated curved templates. Cells on PA-coated, curved surfaces migrated centripetally and were highly aligned compared with the randomly orientated cells on PA-coated, planar templates (right panel). After two weeks in culture, the number of viable cells growing on curved and planar agarose templates was evaluated using the AlamarBlue assay or c) Calcein-AM/PI double staining. Quantification (average ± S.D.) was performed from three independent samples for each condition ($n = 3$). PA-coated surfaces (gray bars) allowed significantly higher number of cells to adhere, migrate, and proliferate compared with corresponding uncoated surfaces (white bars), independently of topography (*** corresponded to $p < 0.001$). Scale bars, 100 µm.

in tissue biofabrication. Subsequently, both curved and planar agarose templates were functionalized with bioactive coatings, namely with a cell adhesive, enzyme-sensitive PA (Figure 1) or Matrigel (Figure S2, Supporting Information). A setup where coating was restricted to the flat region surrounding the curved or planar templates was also used (uncoated controls). Finally, corneal stromal cells were seeded on the flat region surrounding each of the templates (curved and planar), and their growth behavior analyzed.

Both PA and Matrigel coatings were able to provide a stable substrate for corneal stromal cells to adhere and proliferate on the otherwise low-attachment agarose surfaces (Figure 1b; Figure S2, Supporting Information). In addition, coatings allowed cells to migrate, from the flat region on which they were initially seeded, upward toward the apex of the curved templates (Figure 1a,b). Cells were unable to replicate this on uncoated curved templates (Figure 1b), no matter the duration of culture. Furthermore, coatings promoted corneal stromal cell proliferation, independent of surface geometry (Figure 1b; Figure S2, Supporting Information). This was illustrated by the significantly ($p < 0.001$) higher number of cells growing on coated templates compared with uncoated surfaces after two weeks in serum-free culture conditions. Specifically, cells on PA-coated and uncoated curved templates corresponded to 178 ± 4% and 9 ± 3% of the initial cell seed, respectively (Figure 1b). Similarly, cells on Matrigel-coated curved templates corresponded to 205 ± 25% of the initial cell seed (Figure S2, Supporting Information). Coatings were also required to maintain cell adhesion and growth on planar agarose surfaces, with cells on PA-coated and uncoated planar templates corresponding to 207 ± 21% and 22 ± 3% of the initial cell seed, respectively (Figure 1b; Figure S2, Supporting Information). Moreover, coatings were not toxic and preserved high cell viability (>90%) in both curved and planar-coated surfaces (no significant differences between geometries, with $p = 0.17$) (Figure 1c).

Intriguingly, cell migration on curved surfaces was uniformly centripetal, from the bottom/periphery up toward the center/apex of the curved surface template (Figure 1b). These migrating cells were unexpectedly highly organized, and assumed a radial alignment all around the curved surface template (**Figure 2**). This behavior starkly contrasted with the migration pattern on planar templates, where cells moving to the center showed a more expected random orientation (Figure 1b). Moreover, cells grown on curved templates maintained their radial alignment over the entire surface of the curved substrate, initially upon reaching confluence, and up to three months in retinoic acid (RA)-supplemented, serum-free culture conditions. During this period, cells continued to proliferate, deposit ECM, and stratify (Figure 2a). Interestingly, stratified cells assumed a new, prevalently circumferential, orthogonal orientation relative to that of the basal monolayer (Figure 2a). This cell arrangement was observed throughout the template area, from the bottom/periphery to the center/apex of the curved surfaces (Video S1, Supporting Information). In contrast, cells on the flat regions of curved templates (Figure 2a,iii) or migrating and proliferating on planar templates (Figure 2b) presented a more or less random orientation, even after stratification.

Previously, corneal stromal cells grown on PA-coated, planar glass templates were shown to fabricate planar tissue equivalents comprised of large amounts of stroma-characteristic ECM.[18] To recover these tissues intact, the use of the enzyme-sensitive PA was shown to be highly useful. Removal of RA from the serum-free medium allowed corneal stromal cells to resume the expression of matrix metalloproteases (MMPs),[25] which subsequently accumulated in culture[19] and cleaved the cell adhesive PA coating (**Figure 3**a). In the present work, this method allowed the controlled tissue self-release from the PA coating on both curved and planar agarose templates (Figure 3). Importantly, the free-floating, scaffold-, and carrier-free tissues fabricated on curved templates retained their original shape (Figure 3b), with size (12.2 ± 0.2 mm wide, 2.9 ± 0.1 mm deep) and curvature (7.9 ± 0.1 mm radius of curvature at the apex) similar to those of the native cornea.[26] Moreover, tissues endured up to two months of further culture following self-release, with no contraction or shape loss (Figure 3b, right panel), and without the need of crosslinking agents. Curved tissues were also robust enough to be recovered from Matrigel-coated templates using tweezers (Figure S3, Supporting Information). However,

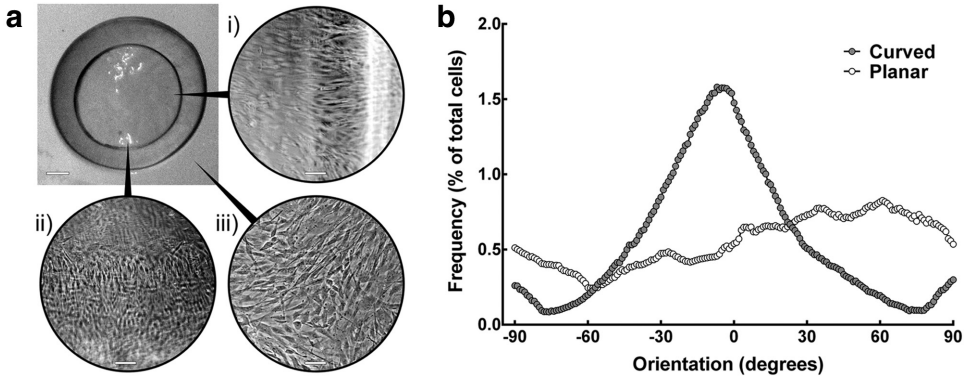

Figure 2. Alignment of cells on PA-coated agarose templates. a) Representative phase-contrast images of the biofabrication setup after six weeks in culture. The PA coating allowed cells to adhere, migrate, proliferate, and deposit large amounts of ECM on curved agarose templates, in serum-free conditions. Cells growing on curved regions of the template showed a uniform organization (i), with higher centripetal and circular anisotropy (ii) compared with the cells on its periphery (flat region) (iii). b) Quantification of cell orientation on curved and planar templates. Cells migrating and proliferating onto curved templates were preferentially aligned along the curvature's radius (gray dots), with some degree of anisotropy (0° and 90°, respectively), whereas cells on planar templates were more randomly oriented (white dots).

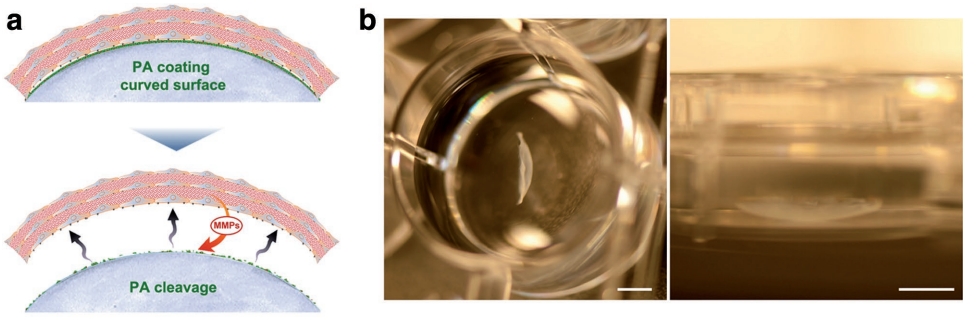

Figure 3. Self-release of tissues biofabricated on PA-coated curved templates. a) Schematic representation of controlled self-release of curved tissues through cleavage of adhesive PA coating. The expression of endogenous MMPs by the tissues was stimulated after removal of RA from the serum-free medium. b) Free-floating curved tissues were easily handled and transferable after self-release from PA-coated templates (left panel), and retained their original shape and integrity for periods up to two months in culture (right panel). Scale bars, 5 mm.

they were more prone to rupture and damage compared with self-released tissues obtained after MMP-controlled degradation of PA coatings. These results supported the idea of using this enzyme-sensitive coating to produce curved templates for the manufacturing of easily recovered, easy-to-handle, cornea-shaped tissues equivalents.

Tissues self-released from PA-coated templates were characterized for their structural, mechanical, compositional, and biofunctional properties. Curved corneal stromal tissue equivalents were shown to be 12.9 ± 2.6 µm thick, and have a relatively smooth topography comprised of a dense mesh of collagen fibrils deposited in a highly aligned pattern (**Figure 4**a, left panel). Specifically, curved tissues were shown to have 72% and 12% of their collagen fibrils oriented within 30° of the tissues' radial and circumferential axes, respectively (Figure S4, Supporting Information). In contrast, planar tissues were comprised of collagen fibril-deposited more or less random orientations (Figure 4a, right panel), with 28% and 38% of fibrils oriented within 30° of the tissues' radial and circumferential axes, respectively (Figure S4, Supporting Information). No significant differences were observed between collagen fibril dimensions (31 ± 2 and 29 ± 3 nm diameter; 61 ± 4 and 58 ± 5 nm *d*-spacing in curved and planar tissues, respectively) (Figure 4a). However, the different collagen anisotropy impacted upon the mechanical properties of the different tissue equivalents. Specifically, the elastic modulus (E) of curved tissues evaluated by atomic force microscopy (AFM) was significantly higher ($p = 0.0001$) to that of their planar counterparts, with an average E of 61 ± 12 and 35 ± 16 MPa for curved and planar tissues, respectively (Figure 4b). The highly ordered arrangement of collagen fibrils was also observed by second harmonic generation (SHG) confocal microscopy (**Figure 5**). The en face SHG forward scatter signals from curved tissues were visualized as long, narrow bundles of linear structures in one prevalent orientation (Figure 5, upper left panel). In contrast, the SHG forward scatter from tissues biofabricated on planar templates (planar tissues) showed short, randomly oriented linear structures (Figure 5, lower left panel). The backscatter SHG signal obtained from curved and planar tissues had a similar appearance to the corresponding forward scatter signals, uniform and randomly oriented, respectively, albeit with overall weaker signal intensity (Figure 5, central panels).

The composition of the corneal stromal tissue equivalents was also evaluated by immunofluorescence confocal

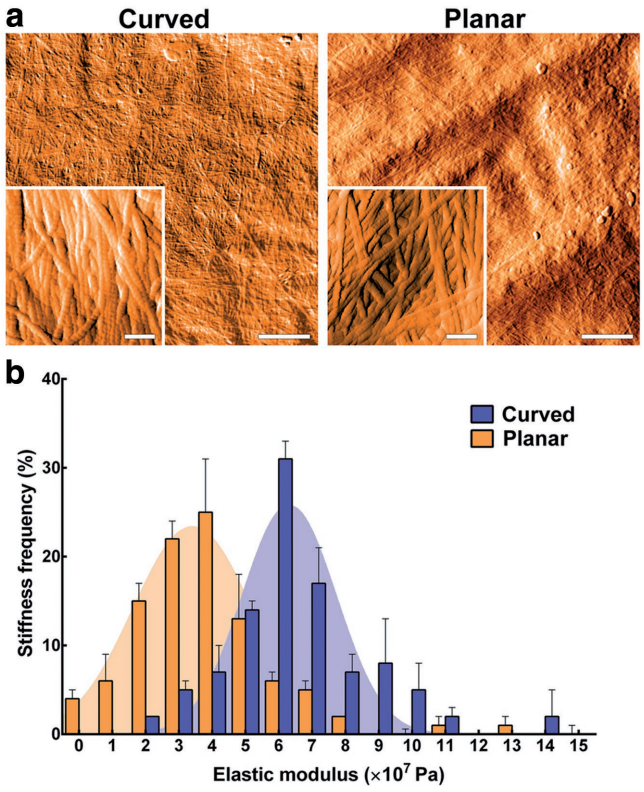

Figure 4. Topographical and biomechanical analyses of curved corneal stromal tissue equivalents. a) Surface topography of tissues biofabricated using curved (left) and planar templates (right panel) analyzed by atomic force microscopy after tissue self-lifting. The surface of curved tissues showed compact deposition of collagen fibrils, predominantly oriented along and perpendicular to the radial axis of the template. In contrast, collagen fibrils of planar tissues were oriented more or less randomly. Images correspond to representative views of three independent samples. Scale bars, 5 µm (0.5 µm in the insets). b) The elastic modulus of curved (blue) and planar tissues (orange bars) was quantified by force–distance spectroscopy, calculated using the Sneddon model and represented as percentage frequency of measured values. The frequency histograms were used to calculate Gaussian curves by nonlinear regression, with a goodness of fit of 0.83 and 0.92, and an elastic modulus of 61 ± 12 and 35 ± 16 MPa for curved (blue area) and planar tissues (orange area), respectively. Data is expressed as average ± SD of three independent experiments ($n = 3$).

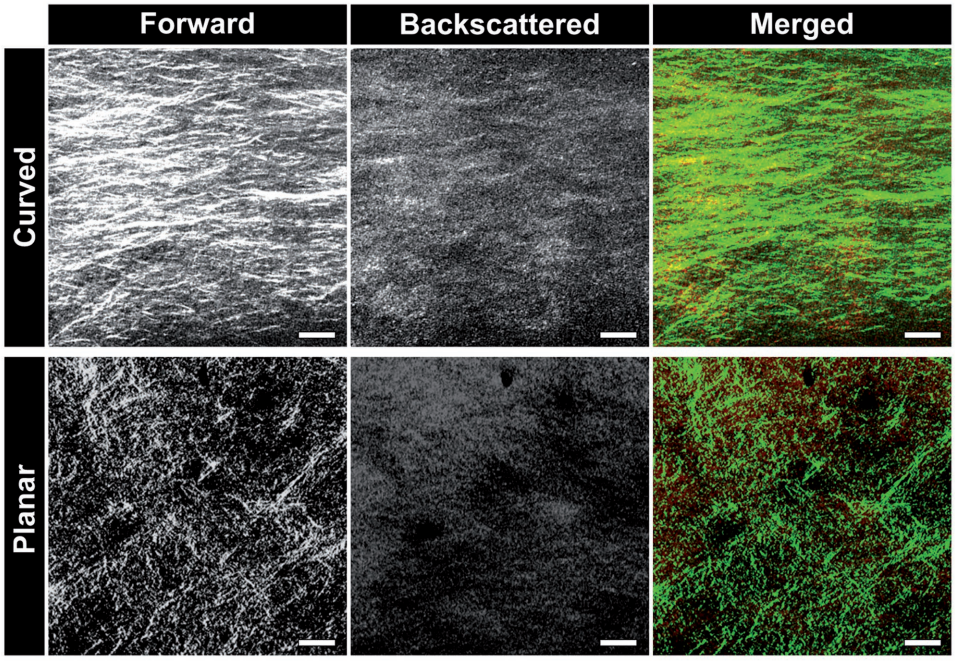

Figure 5. Structure of curved and planar corneal stromal tissue equivalents. Representative SHG images of curved (upper) and planar tissues (lower panels). SHG signals were collected in the forward scattered and backscattered directions. Scale bars, 100 μm.

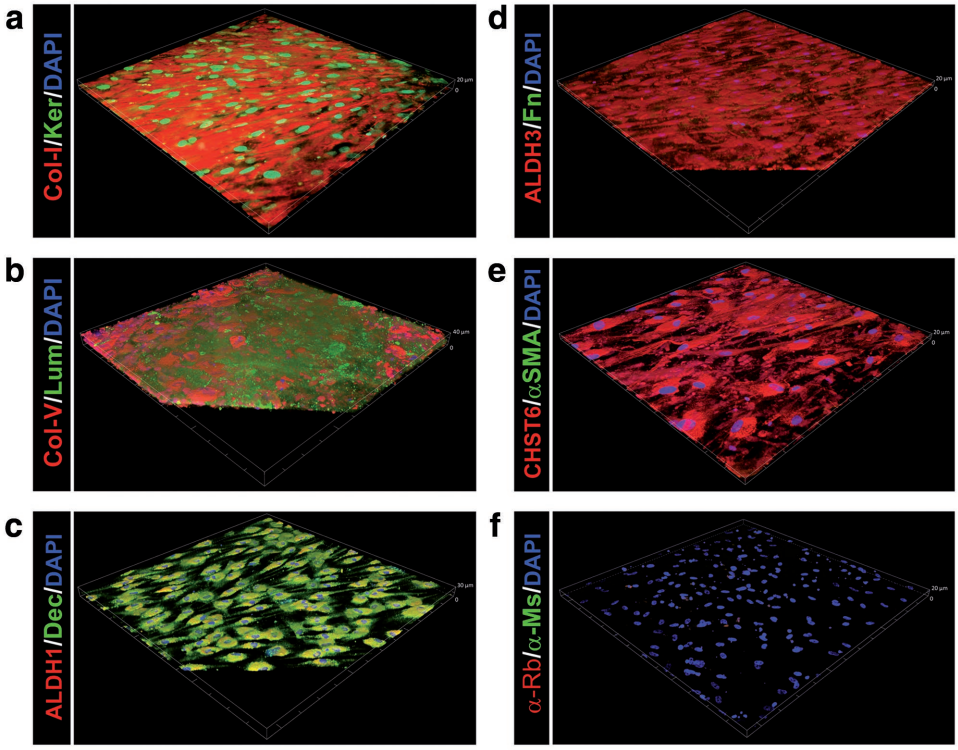

Figure 6. Protein composition of curved corneal stromal tissue equivalents. Curved corneal tissues were imaged by immunofluorescence confocal microscopy, with tridimensional reconstruction of 630 × 630 μm areas of tissue analyzed for expression of a) collagen I and keratocan, b) collagen V and lumican, c) ALDH1 and decorin, d) ALDH3 and fibronectin, and e) CHST6 and αSMA. Cell nuclei were identified by DAPI staining. Signal specificity was evaluated using f) secondary antibody-only controls.

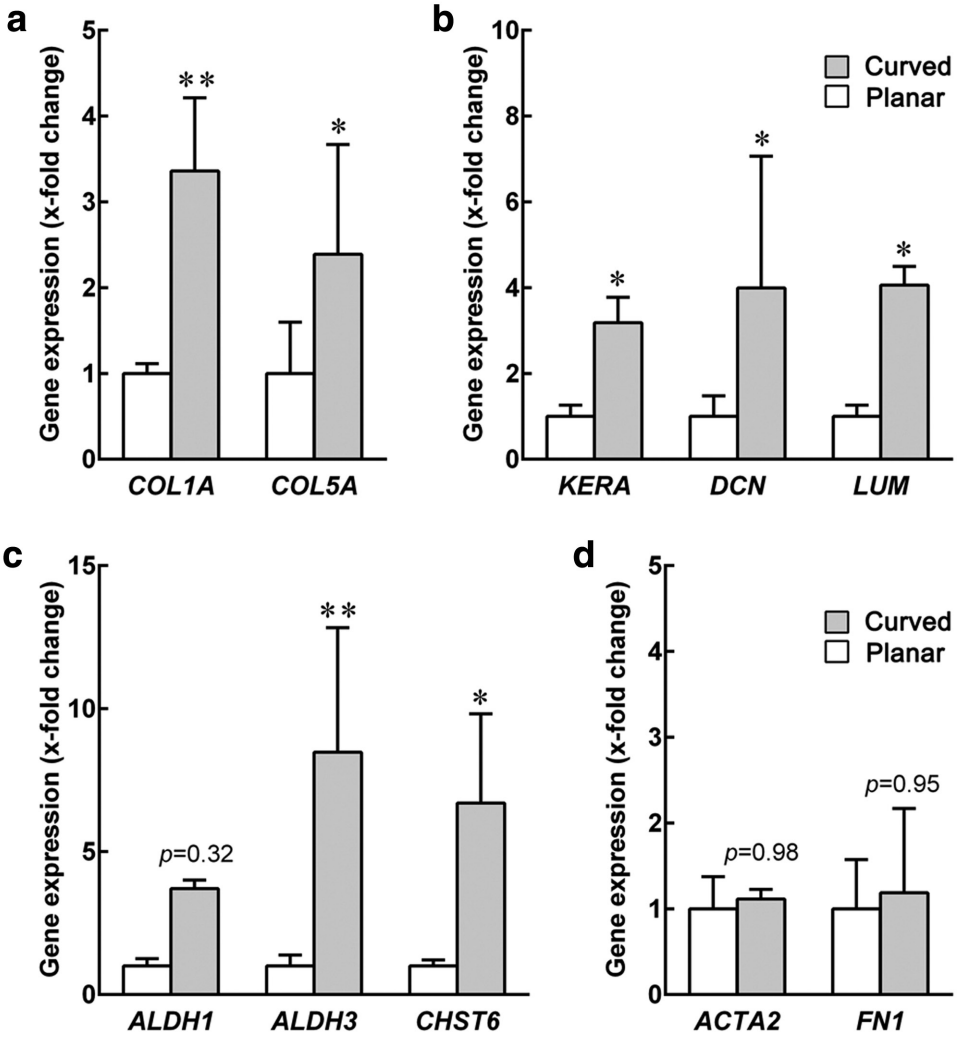

Figure 7. Posttranscriptional composition analysis of corneal stromal tissues. The expression of genes coding for corneal stroma-characteristic markers a) collagen I and V, b) keratocan, decorin, and lumican, c) ALDH1, ALDH3, and CHST6, and d) αSMA and fibronectin were performed by qPCR using total mRNA extracted from curved (gray) and planar corneal tissue equivalents (white bars). Gene expression was normalized relative to the average gene expression of planar tissues. Data (average ± S.D.) were obtained from three independent experiments ($n = 3$; * and ** corresponded to $p < 0.05$ and 0.01, respectively).

microscopy (**Figure 6**). The ECM of curved tissues was shown to be comprised of components characteristic of the native corneal stroma. In particular, these tissues were shown to be comprised of collagen types I and V (Figure 6a,b), as well as proteoglycans such as keratocan, lumican, and decorin (Figure 6a–c), crystallins ALDH1 and ALDH3 (Figure 6c,d), and CHST6 (Figure 6e). In addition, no substantial expression of fibrosis markers fibronectin and αSMA (Figure 6d,e) was detected. Alignment of cells and ECM fibrils could also be observed from the maximum projection of 3D reconstructed confocal micrographs (Figure S5, Supporting Information). Moreover, posttranscriptional composition analysis showed that curved tissues expressed significantly higher levels of these markers compared with their planar counterparts (**Figure 7**). Specifically, genes coding for collagen types I and V (Figure 7a; $p = 0.002$ and 0.03, respectively), keratocan, decorin, and lumican (Figure 7b; $p = 0.012$, 0.033, and 0.029, respectively), and ALDH3 and CHST6 (Figure 7c; $p = 0.003$ and 0.02, respectively) were upregulated in curved tissues, whereas those coding for ALDH1, αSMA, and fibronectin remained unaltered (Figure 7c,d; $p = 0.32$, 0.98, and 0.95, respectively).

The newly formed curved stromal tissue equivalents were also found to be suitable substrates upon which to grow human corneal epithelial cells. When grown for two weeks in CnT-7 medium followed by an additional 2 week period in SHEM and airlifting conditions, epithelial cells populated the entire surface of the curved tissue, creating a stratified epithelium. This epithelium was shown to be comprised of cells positive for CK3 and ZO1 differentiation markers (**Figure 8**a,b), but negative for ΔNp63 and CK15 (Figure 8b,c), two markers characteristic of undifferentiated corneal epithelial cells. In addition, epithelial cells grown on curved tissues were capable of producing specific basement membrane components such as collagen type

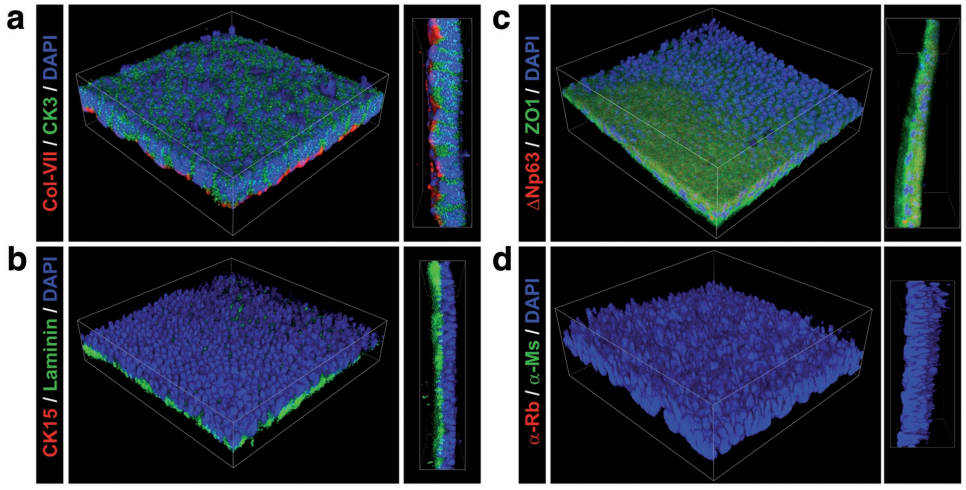

Figure 8. Curved tissues used as substrates for human corneal epithelial cell growth. Epithelial cells isolated from human corneas were grown on curved tissues for two weeks with Cnt-7 medium, followed by an additional two weeks period with SHEM in airlifting conditions, and then imaged by immunofluorescence confocal microscopy. Expression of a) CK3 and collagen VII, b) laminin and CK15, and c) ZO1 and ΔNp63 were analyzed by tridimensional reconstruction of a 300 × 300 µm area. Cell nuclei were identified by DAPI staining. d) Signal specificity was evaluated using secondary antibody-only controls.

VII and laminin, deposited basally between the epithelium and the curved tissue substrate (Figure 8a,c).

3. Discussion

To our knowledge, this is the first study to show that human corneal stromal cells are, by their own, capable of self-organization in response to surface curvature, and in this way fabricate cornea-shaped, highly aligned stromal tissue without the need of carriers, scaffolds, or crosslinking agents. In particular, we showed that curved templates coated with several types of biofunctional materials were able to support the adhesion, migration, and proliferation of corneal stromal cells for prolonged periods in culture. However, most importantly, cells grown on these curved templates deposited large amounts of stroma-characteristic, aligned ECM. The high degree of structural anisotropy of these curved corneal stromal tissue equivalents was consequently shown to be instrumental to their shape, composition, and function.

Curved tissues formed by human corneal stromal cells expressed high levels of ECM components characteristic of the corneal stroma.[1] These included elements of connective tissue such as fibrillar collagen type I and collagen type V, proteoglycans such as keratocan, lumican, and decorin, ALDH1 and ALDH3 crystallins, and CHST6, an enzyme responsible for sulfation of keratan in the cornea.[27] In addition, no evident expression of fibrotic markers such as αSMA stress fibers or fibronectin was observed in curved tissue equivalents. These results supported the notion that cell alignment (in our case induced by curvature) regulates corneal stromal cell phenotype and ECM production.[28] However, curved tissues also showed increased expression of corneal stromal ECM components compared with planar tissues at both posttranscriptional and protein levels, despite their similarly aligned structure.[21] These results match previous work where the application of dome-shaped mechanical strain enhanced the expression of markers characteristic of the corneal stroma, whereas flat-shaped mechanical strain failed to do so.[24]

Moreover, the ability of curved substrates to induce cell alignment allowed the subsequent deposition of ECM to be similarly organized and create compact, robust tissues that retained their original cornea-like shape despite their thinness and subjection to extensive handling. The diameter and *d*-spacing of collagen fibrils comprising the curved tissues closely resembled that observed in the natural cornea,[7] as well as in aligned planar stromal tissue equivalents.[21,29] Furthermore, collagen organization was probably the main factor contributing to the different mechanical properties between curved and planar tissues. Taken together, these structural features suggest that curved tissues generated from curvature-induced cell/collagen alignment have the potential for use as optically suitable, UV-absorbing corneal tissue substitutes.[30]

Furthermore, curved corneal stromal tissue equivalents were shown to support the adhesion, growth, and stratification of human corneal epithelial cells without requiring any feeder layer. This advantage could be due to the maintenance of live corneal stromal cells within the tissues, as suggested previously in high-density collagen gel substrates.[31] Corneal epithelial cells grown on curved tissues were shown to express CK3 and ZO1, both markers of a mature, functional corneal epithelium.[32,33] Moreover, the expression of collagen type VII and laminin on the surface of the stromal tissues demonstrated the capability of the new epithelium to deposit basement membrane components similar to those found in the native cornea.[34] The epithelium grown on curved tissues was negative for the undifferentiated corneal epithelial cell markers CK15 and ΔNp63. We showed in previous works that corneal epithelial cell differentiation and stratification is promoted by stiff (46 ± 22 MPa), anisotropic fibrillar collagen substrates emulating the central areas of the anterior human cornea.[20,21,35] Conversely, softer (26 ± 14 MPa), randomly oriented collagen substrates were

shown to maintain epithelial cells in a slow-cycling, less differentiated state[21] similar to that provided by the native corneal limbus.[36] These results further support the notion that human corneal epithelial cells can sense the different mechanical properties of tissues generated using curved or planar templates, and respond accordingly, by assuming a more or less differentiated phenotype. This represents an important feature and sets up the possibility to rationally design novel templates that control the structure and composition of biofabricated tissues, and through these characteristics, create purposeful substrates capable of defining the phenotype of other cells. For example, PA-coated curved templates could be specifically designed to promote the biofabrication of tissue equivalents with dual properties, e.g., with a stiff, highly anisotropic, curved center capable of promoting epithelial cell differentiation and stratification, and surrounded by an annulus of softer, randomly oriented planar tissue to function as a pseudo-limbus.

In conclusion, the results from this study were in line with previous work where alignment-inducing, biofunctionalized templates enhanced cell and ECM alignment and stratification.[6,18,37] However, this is, to our knowledge, the first example of using surface template curvature alone to elicit cell and ECM self-alignment, and ultimately obtain highly ordered human corneal stromal tissue equivalents with purposeful structural and biological properties intrinsic to such alignment. The molecular mechanisms underlying the cellular response to substrate curvature are possibly related to modulation of the actin cytoskeleton,[38,39] but the specific means are unknown and merit further investigation. From a practical, functional perspective, however, the outcome of this work validates the use of curved templates to fabricate tissue equivalents with appropriate (cornea-shaped) geometries for applications in corneal tissue replacement.

4. Experimental Section

Preparation of Curved Template Surfaces: Ultrapure agarose (#16500-100; Thermo Fisher Scientific, MA, USA) was solubilized in ultrapure water at 5% by heating and then cast between two blown glass contact lenses 10 and 14 mm Ø (Figure S1a, Supporting Information). Agarose constructs ≈13 mm Ø × 3 mm high × 2 mm thick (Figure S1b, Supporting Information) were separated from the molds after solidified and transferred to 12 well tissue plates, convex side up, where they retained their shape. Melted agarose was then poured (0.5 mL per well) around the curved agarose constructs to secure them in place and create an involving flat ring surface (Figure 1a). This method also assured a smooth, continuous transition between the flat and the curved surfaces. The radius and angle of curvature were of ≈8.4 mm and 100°, using the formula for radius and angle of a circular segment, $R = (h/2) + (c^2/8h)$ and $\alpha = 2\arcsin(c/2R)$, respectively, where R corresponds to the radius, α the angle, and h and c the height and chord of the curve, respectively.

Preparation of Coatings: PAs were manufactured as >95% pure trifluoroacetic acid salts (CS Bio, CA, USA), with molecular weight confirmed by electrospray-mass spectrometry, and prepared as previously described.[19] Briefly, the lyophilized PAs C_{16}-TPGPQGIAGQRGDS (MMP/RGDS) and C_{16}-ETTES (ETTES) were weighed separately, solubilized in ultrapure water as a 15:85 mol:mol binary component solution at 1×10^{-2} M, sonicated for 15 min at 55 °C, and maintained at 4 °C overnight to ensure extensive and homogeneous self-assembly, and until further use. Dry PA film coatings were produced by using 1 mL aliquots of PA solutions at 1.25×10^{-3} M in ultrapure water to cover agarose-curved surfaces previously mounted in tissue culture plates, and left to dry overnight (Figure 1a). Planar agarose surfaces of equivalent area were used as controls. Matrigel (#354248; Corning, NY, USA) diluted 1:100 in phosphate buffer saline (PBS) was also used to coat both curved and planar control surfaces. Coatings were washed thrice with sterile PBS prior to cell seeding.

Human Corneal Epithelial and Stromal Cell Isolation and Culture: Corneal tissue by-products were used after grafting procedures in humans, following informed consent and a service-level agreement with the NHS Blood and Transplant service to use leftover human tissue for research. Specifically, cadaveric tissues kept up to one month postisolation from donors (42–76 years old, average ± standard deviation (S.D.) of 60 ± 12 years; male/female donor ratio of 1/3, with no prior history of corneal diseases or ocular trauma), in accordance with Newcastle University and Newcastle-upon-Tyne Hospital Trust Research Ethics Committees guidelines. Human limbal epithelial cells were isolated as previously described.[21] Briefly, corneal limbal rings cut into 4–6 pieces were individually cultured for 7–10 d in 6 well tissue culture plates (Greiner Bio-One, Germany) with 4 mL of CnT-7 medium (CellNTec; Switzerland) at 37 °C and 5% CO_2 in a humidified incubator. Epithelial cells thus isolated were passaged using StemPro Accutase (Thermo Fisher Scientific), expanded in CnT-7 medium, and then used in re-epithelialization experiments. Human corneal stromal cells were isolated and cultured as previously described.[25] Briefly, human corneal limbal rings were shredded and digested in 2 g L^{-1} of collagenase type I (Thermo Fisher Scientific) solution in Dulbecco's modified eagle medium (DMEM)/F12 supplemented with 5% fetal bovine serum (FBS) (Biosera, France) for 5 h at 37 °C, and then incubated with 0.25% Trypsin–EDTA in DMEM/F12 for 10 min. Cells were recovered by centrifugation and expanded in DMEM/F12 with 5% FBS at 37 °C and 5% CO_2. Upon 70–80% confluence, cells were enzyme-dissociated using TrypLE (Thermo Fisher Scientific) and passaged or transferred to serum-free culture medium (SFM) comprising DMEM/F12 with 1×10^{-3} M ascorbic acid, 1% ITS (Sigma-Aldrich), 1% penicillin/streptomycin. Three days before subsequent experiments, SFM was supplemented with all-*trans* RA (Sigma-Aldrich) at 1×10^{-5} M (SFM + RA), to inhibit MMP expression.[25]

Production and Self-Release of Curved Tissue Equivalents: Human corneal stromal cells in SFM + RA were washed twice and then dissociated by trituration using sterile PBS. Cells were then seeded (2×10^4 cells cm^{-2} of the flat area surrounding the curved template surfaces) (Figure 1a) and allowed to proliferate and migrate upward upon the coated and uncoated surfaces toward the center (apex) of the curved templates (Figure 1a). Cells were similarly seeded on the periphery of planar templates and allowed to migrate toward their center. Cells and corresponding ECM deposited during the 90 d culture in SFM + RA were analyzed using a Nikon Eclipse inverted microscope (Nikon, Japan) coupled with a Jenoptik CCD camera (Jenoptik AG, Germany) to assess the impact of template curvature on cell number and alignment. Cell number was also evaluated by the AlamarBlue viability assay (Thermo Fisher Scientific). Briefly, cultures were incubated with resazurin reagent diluted 1:10 in SFM + RA for 4 h at 37 °C, with 0.1 mL supernatant aliquots sampled in triplicate for fluorescence emission at 590 nm. Cell number was calculated by interpolation using a standard curve for the fluorescence values of 1, 2, 4, 6, 8, and 10×10^4 cells. Corneal tissues grown on PA-coated templates were subsequently retrieved as previously described,[19] to enable further structural characterization of the tissue and demonstrate ease of manufacture for future applications. Briefly, tissues were washed three times with sterile PBS and then maintained in SFM without RA supplementation, allowing cells to resume MMP expression. After 3 d, tissue-derived MMPs were able to cleave the cell adhesive PA coating, and subsequently elicit tissue self-release. These self-lifting, auto-generated corneal stromal tissue equivalents were recovered from both curved and planar templates. Stromal tissue equivalents grown on Matrigel were recovered by carefully peeling the tissue using pointed bent tweezers. All experiments were performed three independent times ($n = 3$).

Topographic Analysis of Tissue Equivalents Grown on Curved Templates: The topography of the tissue equivalents was analyzed by calculating the radius of curvature, as described above. Tissue surface nanotopography

analysis was performed by static force mode using an Easyscan 2-controlled atomic force microscope (AFM) (Nanosurf, Switzerland) equipped with soft contact-mode cantilevers (ContAl-G; BudgetSensors, Bulgaria) with a 13 kHz resonant frequency, and nominal spring constant of 0.2 N m^{-1}. Tissues grown on curved and planar templates were mounted onto glass slides covered with Parafilm M (Bemis, WI, USA) to minimize sample displacement and drift. The topography of each tissue was determined using five independent samples, with 2048 × 2048 two-directional lines scanned at 10 µm s^{-1} at 5 nV, and with a P- and I-gain of 1, line-wise and tilt correction process using the Scanning Probe Image Processor (SPIP) software package. Collagen fibril dimensions, orientation, and distribution were analyzed using the OrientationJ plugin from ImageJ v1.46. The angle of orientation of 100 × independent collagen fibrils was calculated relative to the direction of the circumferential radius of tissue equivalents produced on curved templates, pooled in 1° angle bins between –90° and 90°, with 0° and 90° being parallel and perpendicular to the radius, respectively, and the negative and positive values indicating orientation handedness. For tissues formed on flat templates, fibril orientation was calculated using a fixed direction as the 0° reference, with similar angle binning. All experiments were performed three independent times ($n = 3$).

Culture of Human Corneal Epithelial Cells on Curved Tissue Equivalents: Corneal stromal tissue equivalents self-released from PA-coated curved templates were washed three times with sterile PBS, mounted in Transwell tissue culture inserts (Corning, NY, USA), and then seeded with human corneal epithelial cells at a density of 5×10^4 cells cm^{-2}. Epithelial cells were cultured for two weeks with CnT-7 medium, followed by an additional two weeks period with supplemented hormonal epithelial medium (DMEM/F12 with 5% FBS, 2×10^{-6} g L^{-1} mouse EGF, 1% ITS, 0.5% dimethyl sulfoxide, 5×10^{-2} g L^{-1} hydrocortisone, 1×10^{-9} M cholera toxin (Sigma-Aldrich), and 1% penicillin/streptomycin) and airlifting.

Immunofluorescence Confocal Microscopy Analysis of Tissue Equivalents: Corneal stromal tissue equivalents were fixed in 4% paraformaldehyde for 20 min, washed two times with 0.1% Triton X-100 (Sigma-Aldrich) in PBS for 5 min, blocked in wash solution containing 2% BSA for 1 h, and incubated with primary antibodies diluted 1:500 in blocking solution for 2 h: goat anticollagen I (ab19811; Abcam, UK) or antidecorin (PC673; Merck), rabbit antikeratocan (sc-66941; Santa Cruz Biotechnology), anticollagen V (ab7046; Abcam), anti-ALDH1 (ab23375; Abcam), anti-ALDH3 (PA5-15004; Thermo Fisher Scientific) or anti-CHST6 (ab154332; Abcam), or mouse antilumican (kindly provided by Dr. Bruce Caterson, Cardiff School of Biosciences, Cardiff, UK), antifibronectin (VPF705; Vector Laboratories, UK), or anti-αSMA (VPS281; Vector Laboratories). Tissues were then washed thrice for 5 min with wash solution and incubated with corresponding Alexa 594- or Alexa 488-conjugated secondary antibodies (R-37119, A-11029, and A-11055; Thermo Fisher Scientific) for 1 h. Corneal epithelial cells grown on tissue equivalents were stained using the following primary antibodies: rabbit antiCK15 (ab52816; Abcam), anticollagen VII (ab93350; Abcam), or anti-ΔNp63 (sc-8343; Santa Cruz Biotechnology), mouse anticytokeratin 3 (sc-80000; Santa Cruz Biotechnology, TX, USA) or antilaminin-1 (MA1-21194; Thermo Fisher Scientific), or goat anti-ZO1 (STJ71854; St John's Laboratory, UK). All tissues were finally washed twice with wash solution, mounted in VectaShield antifade medium containing DAPI (H-1200; Vector Laboratories), and imaged using an A1R confocal microscope (Nikon), using constant illumination and capture parameters, with postcapture analysis performed using both the NIS-Elements (Nikon) and ImageJ v1.46 software.

Quantitative PCR (qPCR) of Tissue Equivalents: qPCR was performed using the default thermal profile of the Eco Real-Time polymerase chain reaction (PCR) System (Illumina, CA, USA), as previously described.[40] Briefly, amplification was performed using a 40 × three-step cycle (10 s denaturation, 95 °C; 30 s annealing, 60 °C; and 15 s elongation, 72 °C), and the relative expression of the human *COL1A*, *COL5A*, *KERA*, *DCN*, *LUM*, *ALDH1*, *ALDH3*, *CHST6*, *ACTA2*, and *FN1* genes was calculated by the comparative threshold cycle (CT) (Eco Software v3.1, Illumina), normalized to the expression of the *POLR2A* housekeeping gene, and represented as fold-change relative to the planar tissue equivalents' corresponding expression average. All experiments were performed three times, independently ($n = 3$).

SHG Imaging: The collagen organization of curved and planar tissues was investigated using nonlinear optical second-harmonic generation (SHG) imaging. The samples were mounted and placed under a Zeiss 510 LSM (LSM 510; Carl Zeiss AG, Germany) and SHG signals were generated using a Chameleon mode-locked Titanium–Sapphire femtosecond laser (Coherent Incorporated, CA, USA) tuned to 820 nm, which provided a strong collagen signal. Forward and Backscatter SHG signals were collected by the LSM's detector array in two separate channels. All samples were examined using a 40×/NA 1.2 Zeiss ApoChromat objective at a resolution of 512 × 512 pixels per image and with a lateral resolution of 44 µm per pixel. Image stacks of 1 or 2 µm *z*-axis step size were obtained to generate 3D data sets using the LSM Image Examiner (Carl Zeiss AG). During each image stack acquisition, each line was scanned and averaged four times to counteract noise.

Statistical Analysis: For cell quantification, structural orientation, and compositional analysis, the differences between groups were determined using one-way analysis of variance (ANOVA) followed by Bonferroni's multiple comparison post hoc test. Significance between groups was established for $p < 0.05$, 0.01, and 0.001, with a 95% confidence interval. For all assays, error bars represented the S.D. of the mean, analyzed a priori for normality and homogeneity of variance (D'Agostino–Pearson's and Bartlett's tests, respectively). The frequency distribution of elastic modulus of both curved and planar tissues was tested for correlation, fit (with a $R^2 = 0.92$ and 0.83, respectively) to Gaussian curves using a nonlinear least-squares regression model, and then analyzed for independence using the Chi-squared test. Statistical analysis was performed using GraphPad Prism v6.01 software.

Supporting Information

Supporting Information is available from the Wiley Online Library or from the author.

Acknowledgements

This work was supported by the Biotechnology and Biological Sciences Research Council UK (Grant references BB/N021576/1 and BB/M025349/1).

Conflict of Interest

The authors declare no conflict of interest.

Keywords

biofabrication, collagen alignment, corneal stromal tissue equivalents, curved tissue templating, tissue self-release

Received: July 14, 2017
Revised: August 30, 2017
Published online: October 20, 2017

[1] C. E. Ghezzi, J. Rnjak-Kovacina, D. L. Kaplan, *Tissue Eng., Part B* **2015**, *21*, 278.
[2] R. M. Gouveia, C. J. Connon, in *Biomaterials and Regenerative Medicine in Ophthalmology* (Eds: T. Chirila, D. Harkin), Woodhead Publishing, Elsevier, UK **2016**, Ch. 7.
[3] P. Fagerholm, N. S. Lagali, J. A. Ong, K. Merrett, W. B. Jackson, J. W. Polarek, E. J. Suuronen, Y. W. Liu, I. Brunette, M. Griffith, *Biomaterials* **2014**, *35*, 2420.

[4] H. J. Levis, J. Menzel-Severing, R. A. Drake, J. T. Daniels, *Curr. Eye Res.* **2013**, *38*, 41.
[5] M. Rafat, F. F. Li, P. Fagerholm, N. S. Lagali, M. A. Watsky, R. Munger, T. Matsuura, M. Griffith, *Biomaterials* **2008**, *29*, 3960.
[6] J. Wu, J. Rnjak-Kovacina, Y. Q. Du, M. L. Funderburgh, D. L. Kaplan, J. L. Funderburgh, *Biomaterials* **2014**, *35*, 3744.
[7] A. Daxer, K. Misof, B. Grabner, A. Ettl, P. Fratzl, *Invest. Ophthalmol. Visual Sci.* **1998**, *39*, 644.
[8] J. Burck, S. Heissler, U. Geckle, M. F. Ardakani, R. Schneider, A. S. Ulrich, M. Kazanci, *Langmuir* **2013**, *29*, 1562.
[9] N. Saeidi, K. P. Karmelek, J. A. Paten, R. Zareian, E. DiMasi, J. W. Ruberti, *Biomaterials* **2012**, *33*, 7366.
[10] P. Kumar, A. Satyam, X. Fan, E. Collin, Y. Rochev, B. J. Rodriguez, A. Gorelov, S. Dillon, L. Joshi, M. Raghunath, A. Pandit, D. I. Zeugolis, *Sci. Rep.* **2015**, *5*, 8729.
[11] J. Torbet, M. Malbouyres, N. Builles, V. Justin, M. Roulet, O. Damour, A. Oldberg, F. Ruggiero, D. J. Hulmes, *Biomaterials* **2007**, *28*, 4268.
[12] A. Tenboll, B. Darvish, W. Hou, A. S. Duwez, S. J. Dixon, H. A. Goldberg, B. Grohe, S. Mittler, *Langmuir* **2010**, *26*, 12165.
[13] N. Saeidi, E. A. Sander, R. Zareian, J. W. Ruberti, *Acta Biomater.* **2011**, *7*, 2437.
[14] J. Wu, Y. Q. Du, M. M. Mann, E. Z. Yang, J. L. Funderburgh, W. R. Wagner, *Tissue Eng., Part A* **2013**, *19*, 2063.
[15] D. Karamichos, M. L. Funderburgh, A. E. K. Hutcheon, J. D. Zieske, Y. Q. Du, J. Wu, J. L. Funderburgh, *PLoS One* **2014**, *9*, e86260.
[16] J. Wu, Y. Du, S. C. Watkins, J. L. Funderburgh, W. R. Wagner, *Biomaterials* **2012**, *33*, 1343.
[17] T. Kobayashi, K. Kan, K. Nishida, M. Yamato, T. Okano, *Biomaterials* **2013**, *34*, 9010.
[18] R. M. Gouveia, V. Castelletto, S. G. Alcock, I. W. Hamley, C. J. Connon, *J. Mater. Chem. B* **2013**, *1*, 6157.
[19] R. M. Gouveia, V. Castelletto, I. W. Hamley, C. J. Connon, *Tissue Eng., Part A* **2015**, *21*, 1772.
[20] R. M. Gouveia, I. W. Hamley, C. J. Connon, *J. Mater. Sci.: Mater. Med.* **2015**, *26*, 242.
[21] R. M. Gouveia, E. Gonzalez-Andrades, J. C. Cardona, C. Gonzalez-Gallardo, A. M. Ionescu, I. Garzon, M. Alaminos, M. Gonzalez-Andrades, C. J. Connon, *Biomaterials* **2017**, *121*, 205.
[22] F. Li, D. Carlsson, C. Lohmann, E. Suuronen, S. Vascotto, K. Kobuch, H. Sheardown, R. Munger, M. Nakamura, M. Griffith, *Proc. Natl. Acad. Sci. USA* **2003**, *100*, 15346.
[23] S. Li, Y. Han, H. Lei, Y. Zeng, Z. Cui, Q. Zeng, D. Zhu, R. Lian, J. Zhang, Z. Chen, J. Chen, *Sci. Rep.* **2017**, *7*, 777.
[24] W. Zhang, J. Chen, L. J. Backman, A. D. Malm, P. Danielson, *Adv. Healthcare Mater.* **2017**, *6*, 1601238.
[25] R. M. Gouveia, C. J. Connon, *Invest. Ophthalmol. Visual Sci.* **2013**, *54*, 7483.
[26] M. Dubbelman, V. A. Sicam, G. L. van der Heijde, *Vision Res.* **2006**, *46*, 993.
[27] E. Di Iorio, V. Barbaro, N. Volpi, M. Bertolin, B. Ferrari, A. Fasolo, R. Arnaldi, P. Brusini, G. Prosdocimo, D. Ponzin, S. Ferrari, *Exp. Eye Res.* **2010**, *91*, 293.
[28] W. M. Petroll, M. Miron-Mendoza, *Exp. Eye Res.* **2015**, *133*, 49.
[29] F. N. Syed-Picard, Y. Du, A. J. Hertsenberg, R. Palchesko, M. L. Funderburgh, A. W. Feinberg, J. L. Funderburgh, *J. Tissue Eng. Regener. Med.* **2017**, https://doi.org/10.1002/term.2363.
[30] Y. Chen, D. C. Thompson, V. Koppaka, J. V. Jester, V. Vasiliou, *Prog. Retinal Eye Res.* **2013**, *33*, 28.
[31] A. K. Kureshi, M. Dziasko, J. L. Funderburgh, J. T. Daniels, *Sci. Rep.* **2015**, *5*, 16186.
[32] Y. Ban, A. Dota, L. J. Cooper, N. J. Fullwood, T. Nakamura, M. Tsuzuki, C. Mochida, S. Kinoshita, *Exp. Eye Res.* **2003**, *76*, 663.
[33] U. Schlotzer-Schrehardt, F. E. Kruse, *Exp. Eye Res.* **2005**, *81*, 247.
[34] U. Schlotzer-Schrehardt, T. Dietrich, K. Saito, L. Sorokin, T. Sasaki, M. Paulsson, F. E. Kruse, *Exp. Eye Res.* **2007**, *85*, 845.
[35] S. M. Thomasy, V. K. Raghunathan, M. Winkler, C. M. Reilly, A. R. Sadeli, P. Russell, J. V. Jester, C. J. Murphy, *Acta Biomater.* **2014**, *10*, 785.
[36] E. Di Iorio, V. Barbaro, A. Ruzza, D. Ponzin, G. Pellegrini, M. De Luca, *Proc. Natl. Acad. Sci. USA* **2005**, *102*, 9523.
[37] S. L. Wilson, I. Wimpenny, M. Ahearne, S. Rauz, A. J. El Haj, Y. Yang, *Adv. Funct. Mater.* **2012**, *22*, 3641.
[38] H. Miyoshi, T. Adachi, *Tissue Eng., Part B* **2014**, *20*, 609.
[39] M. J. Dalby, N. Gadegaard, R. O. Oreffo, *Nat. Mater.* **2014**, *13*, 558.
[40] F. Z. Abidin, R. M. Gouveia, C. J. Connon, *Organogenesis* **2015**, *11*, 122.